Recommended Implementation of Arterial Spin-Labeled Perfusion MRI for Clinical Applications: A Consensus of the ISMRM Perfusion Study Group and the European Consortium for ASL in Dementia

David C. Alsop,[1] John A. Detre,[2] Xavier Golay,[3] Matthias Günther,[4,5,6] Jeroen Hendrikse,[7] Luis Hernandez-Garcia,[8] Hanzhang Lu,[9] Bradley J. MacIntosh,[10,11] Laura M. Parkes,[12] Marion Smits,[13] Matthias J. P. van Osch,[14] Danny J. J. Wang,[15] Eric C. Wong,[16]* and Greg Zaharchuk[17]†

This review provides a summary statement of recommended implementations of arterial spin labeling (ASL) for clinical applications. It is a consensus of the ISMRM Perfusion Study Group and the European ASL in Dementia consortium, both of whom met to reach this consensus in October 2012 in Amsterdam. Although ASL continues to undergo rapid technical development, we believe that current ASL methods are robust and ready to provide useful clinical information, and that a consensus statement on recommended implementations will help the clinical community to adopt a standardized approach. In this review, we describe the major considerations and trade-offs in implementing an ASL protocol and provide specific recommendations for a standard approach. Our conclusion is that as an optimal default implementation, we recommend pseudo-continuous labeling, background suppression, a segmented three-dimensional readout without vascular crushing gradients, and calculation and presentation of both label/control difference images and cerebral blood flow in absolute units using a simplified model. **Magn Reson Med 73:102–116, 2015. © 2014 Wiley Periodicals, Inc.**

Key words: arterial spin labeling; perfusion; cerebral blood flow

[1]Department of Radiology, Beth Israel Deaconess Medical Center and Harvard Medical School, Boston, Massachusetts, USA.

[2]Departments of Neurology and Radiology, University of Pennsylvania, Philadelphia, Pennsylvania, USA.

[3]Department of Brain Repair and Rehabilitation, UCL Institute of Neurology, London, UK.

[4]Fraunhofer MEVIS, Bremen, Germany.

[5]University Bremen, Bremen, Germany.

[6]Mediri GmbH, Heidelberg, Germany.

[7]Department of Radiology, University Medical Center Utrecht, Utrecht, The Netherlands.

[8]FMRI Laboratory, Department of Biomedical Engineering, University of Michigan, Ann Arbor, Michigan, USA.

[9]Advanced Imaging Research Center, UT Southwestern Medical Center, Dallas, Texas, USA.

[10]Department of Medical Biophysics, University of Toronto, Toronto, Canada.

[11]Department of Physical Sciences, Sunnybrook Research Institute, Toronto, Canada.

[12]Centre for Imaging Science, Institute of Population Health, Faculty of Medical and Human Sciences, University of Manchester, Manchester, UK.

[13]Department of Radiology, Erasmus MC, University Medical Centre Rotterdam, Rotterdam, The Netherlands.

[14]C. J. Gorter Center for High Field MRI, Department of Radiology, Leiden University Medical Center, Leiden, The Netherlands.

[15]Department of Neurology, University of California Los Angeles, Los Angeles, California, USA.

[16]Departments of Radiology and Psychiatry, University of California San Diego, La Jolla, California, USA.

[17]Department of Radiology, Stanford University, Stanford, California, USA.

Grant sponsor: NIH; Grant numbers: P41 EB015893, R01 EB014922, R01 NS081077, R01 NS066506, R01 MH084021, R01 MH080729, and R21 EB013821; Grant sponsor: Dutch Heart Association; Grant number: 2010B274.

*Correspondence to: Eric C. Wong, UCSD Center for Functional MRI, 9500 Gilman Drive, Mail Code 0677, La Jolla, CA 92093-0677. E-mail: ecwong@ucsd.edu

†With endorsement by the ASNR, the ASFNR, and 245 individual investigators. Endorsement list available as Supporting Information.

Additional Supporting Information may be found in the online version of this article.

Authors are listed in alphabetical order.

Received 2 October 2013; revised 8 February 2014; accepted 10 February 2014

DOI 10.1002/mrm.25197
Published online 8 April 2014 in Wiley Online Library (wileyonlinelibrary.com).

INTRODUCTION

Arterial spin-labeled (ASL) perfusion MRI permits noninvasive quantification of blood flow, which is an important physiological parameter. Disorders of perfusion such as stroke account for much of medical morbidity in industrialized nations, and blood flow alterations also commonly accompany other pathophysiological changes such as cancer, epilepsy, and neurodegenerative diseases. Through a number of methodological advances, ASL MRI has evolved from initial single slice feasibility studies using lengthy acquisitions to the current state-of-the-art whereby high-quality whole brain perfusion images can be obtained in a few minutes of scanning. ASL MRI has been validated extensively against other methods that use exogenous contrast agents, such as ^{15}O-PET (1,2), and ASL implementations are now commercially available on all major MRI platforms, with demonstrated reproducibility in multicenter studies (3,4). Clinical applications of ASL perfusion MRI in the brain have recently been reviewed (5,6), and applications of ASL MRI outside the brain are now under development.

The goal of this review is to provide current recommendations for the implementation of ASL perfusion MRI for clinical applications. Since the inception of ASL more than 20 years ago (7), the quality of ASL-derived perfusion maps has reached a level that makes the method useful for many clinical and research applications (Fig. 1). However, 20+ years of technical development has left potential users with a plethora of labeling schemes, readout options, and models to quantify

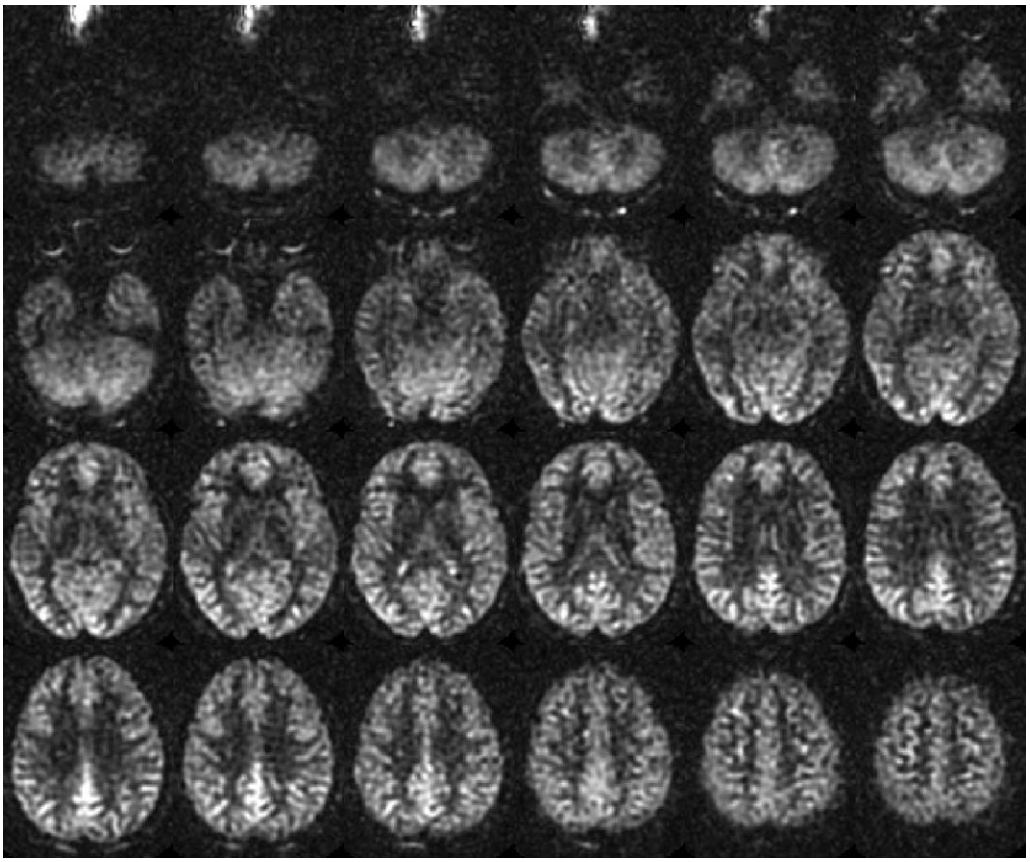

FIG. 1. Example of whole brain ASL imaging of cerebral blood flow at 3T using the recommended parameters in a normal subject, highlighting the typical image quality and expected contrast between gray and white matter.

perfusion, or cerebral blood flow (CBF) in the brain, making it difficult for a clinician or new researcher to decide what method is most appropriate for each application. We believe that this overabundance of choices is an impediment to the acceptance of ASL by the clinical community, complicating the implementation of ASL in standard clinical care, comparisons between sites, and the establishment of meaningful clinical trials. Furthermore, it is likely that this wide diversity of techniques has slowed implementation and adoption of ASL by MRI vendors, thereby limiting its availability.

In 2011–2012, the Perfusion Study Group of the International Society for Magnetic Resonance in Medicine (ISMRM) and the European consortium ASL in Dementia (AID) (funded through a grant from the European Union COST agency as COST Action BM1103) both recognized that a clear set of recommendations was needed in order to encourage the adoption and improve the utility of ASL, and resolved to collaborate on a consensus statement of current recommendations (the present review). In October 2012, an ISMRM workshop on perfusion imaging and an AID Action Workshop were held on consecutive days in Amsterdam, with a primary focus on open and inclusive discussion of current recommendations for implementation of ASL for clinical applications. A draft of this document was further discussed at a Virtual Meeting of the ISMRM Perfusion Study Group in August 2013. This document reports on the consensus that was reached during those meetings. It is cosigned by the participants, as well as additional members of the ISMRM Perfusion Study Group and the COST-sponsored AID Consortium, and is further endorsed by the American Society of Neuroradiology and the American Society of Functional Neuroradiology. A complete list of endorsements is available in the Supporting Information online.

Although ASL MRI can be used to study any organ, this recommendation focuses exclusively on ASL in the brain, which to date is the most common and well-studied application. Recommendations will be discussed in seven sections covering the main aspects of ASL: 1) hardware considerations; 2) ASL approaches; 3) time delay between labeling and imaging; 4) background suppression; 5) readout approaches; 6) postprocessing methods; and 7) ASL in the clinical setting.

ASL is still a rapidly developing field, both in terms of technical innovation and applications. In no way is this review intended to suggest that there is only one or a few correct ways to perform ASL, nor should it have the effect of slowing innovation or development of the field. Rather, it is intended to document the current recommendations for the optimal use of ASL in clinical applications in order to encourage implementation of robust ASL methods and promote uniformity of data across scanner types, sites, and studies. We expect that as ASL methods continue to develop, these recommendations should be updated, and recommend that this consensus

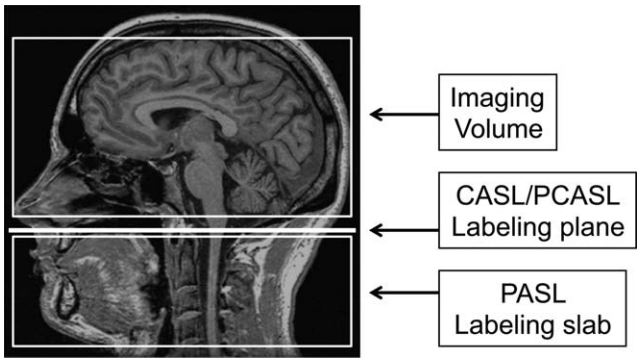

FIG. 2. Schematic diagram of imaging and labeling regions for CASL/PCASL and PASL. In CASL/PCASL, labeling occurs as blood flow through a single labeling plane, while in PASL, a slab of tissue, including arterial blood, is labeled.

statement be revised on a regular basis, perhaps every 3–5 years.

A BRIEF OVERVIEW OF ASL

ASL (7,8) uses arterial blood water as an endogenous diffusible tracer by inverting the magnetization of the blood using radiofrequency (RF) pulses. After a delay to allow for labeled blood to flow into the brain tissue, labeled images are acquired that contain signal from both labeled water and static tissue water (9). Separate control images are also acquired without prior labeling of arterial spins, and the signal difference between control and labeled images provides a measure of labeled blood from arteries delivered to the tissue by perfusion. The lifetime of the tracer is governed by the longitudinal relaxation time of blood, which is in the range of 1300–1750 ms at clinical field strengths (10,11). Many implementation choices of ASL are influenced by the fact that this lifetime is similar to the transport time from the labeling position to the tissue (known as the arterial transit time [ATT]). The fundamental trade-off is that a short delay does not allow for complete delivery of the labeled blood water to the tissue, whereas a long delay results in strong T_1 decay and therefore reduced signal-to-noise ratio (SNR). The ATT varies between individuals, regionally, and between healthy and pathological tissue (4,12).

Hardware Considerations

A field strength of 3T is recommended when available, though satisfactory results can be obtained at 1.5T. The advantage of increased field strength is higher SNR, which results from a combination of higher intrinsic SNR and longer T_1 (13). The lower SNR at 1.5T can be compensated for by a combination of decreased spatial resolution and/or increased scan time. The recommended parameters given below are valid for both 3T and 1.5T.

The use of multichannel receive head coils with eight or more channels is advised for ASL. Multichannel head coils not only increase the SNR of the MRI images, but also enable the use of parallel imaging acceleration (14,15), which can be exploited to decrease the echo time and the total readout duration (16). Without the use of multichannel head coils, the user is advised to lower the spatial resolution to compensate for the lower SNR.

Because ASL is a subtractive technique it is sensitive to motion, and segmented three-dimensional (3D) acquisition methods (see the "Readout Approaches" section later in this review) incur additional motion sensitivity. Therefore, patient motion should be minimized as much as possible. Motion sensitivity can also be partially mitigated by the use of background suppression, which provides strong motivation for the use of that feature (see the "Background Suppression" section later in this review).

ASL Labeling Approaches

ASL labeling approaches can be grouped into three types: continuous labeling (7,8,17), pulsed labeling (18–20), and velocity selective labeling (21). Velocity selective ASL is currently considered to be in development and requires additional validation for routine clinical care; therefore, only continuous and pulsed labeling are discussed here.

Pulsed and continuous ASL labeling methods differ fundamentally in both the spatial extent and the duration of the labeling (Figs. 2 and 3), and these differences give rise to the strengths and weaknesses of each approach. In the continuous ASL, labeling occurs over a long period, typically 1–3 s, as blood flows through a single labeling plane and is inverted by an effective continuous RF energy. This process is known as flow-driven adiabatic inversion. There are two distinct forms of continuous ASL: 1) continuous ASL (CASL), in which one single, long label is applied (8), and 2) pseudo-continuous ASL (PCASL), in which 1000 or more shaped RF pulses are applied at a rate of approximately one per millisecond (17). CASL was originally implemented for human use as a single slice technique (22) but was later extended to multislice imaging (23). Both forms of CASL constitute long label scenarios, but PCASL provides superior labeling efficiency and is compatible with modern body coil RF transmission hardware that is now ubiquitous on clinical MRI scanners. Accordingly, PCASL is the continuous ASL labeling scheme that is recommended for clinical imaging and is thus referred to henceforth when discussing CASL. In contrast, pulsed

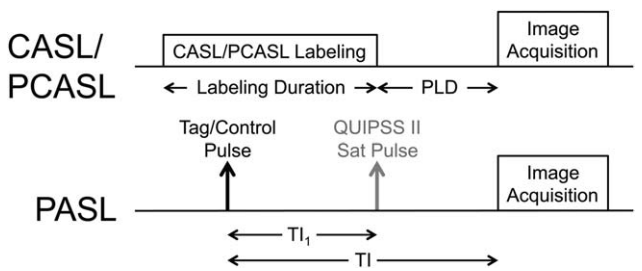

FIG. 3. Timing diagram for CASL/PCASL and PASL. For QUIPSS II PASL, TI_1 is the bolus duration, and is analogous to the labeling duration in CASL/PCASL. The PLD in CASL/PCASL is analogous to the quantity ($TI-TI_1$) in QUIPSS II PASL.

ASL (PASL) uses a single short pulse or a limited number of pulses, with a total duration of typically 10–20 ms, to invert a thick slab of arterial water spins (20,24,25). The SNR of the PCASL approach is higher than that of PASL for two reasons. First, the temporal duration of the labeled bolus is longer in PCASL, and this is proportional to the volume of labeled blood that is delivered to the tissue, translating to an increase in SNR. In PASL, the bolus is derived from a labeling slab that is 10–20 cm thick, which is limited by the spatial coverage of the transmit RF coil. The arteries supplying blood to the brain have mean velocities of ~20 cm/s, so the temporal duration of the generated PASL bolus is typically 1 s or less. This smaller bolus translates to a shorter labeling duration and consequently lower SNR in PASL compared with CASL. Second, even for a bolus of equal temporal duration, and correction for lower labeling efficiency, the labeled magnetization delivered using PCASL is higher than that of PASL. For both methods, a spatial gap exists between the labeling and imaging regions. The labeling plane for CASL is typically in approximately the same location as the distal end of the labeling slab in PASL (Fig. 2). For PASL, a single pulse simultaneously inverts the entire labeled bolus, and this bolus decays with time constant T_1 for the entire time between the inversion pulse and image acquisition. For CASL, blood is inverted as it passes through the labeling plane, and therefore the bolus is, on average, inverted later in time than in PASL, leading to less T_1 decay, and a larger ASL signal (19).

Ease of use and adequate SNR are two critical considerations in the implementation of robust clinical perfusion imaging using ASL. We therefore recommend PCASL as the workhorse labeling approach with ASL images collected at a single postlabeling delay (PLD). As clinicians gain and share experience, it will be possible to adjust the ASL acquisition to account for issues that arise in cerebrovascular and/or neurological studies, such as prolonged or heterogeneous blood transit times. In these cases, multiple (PLD) values can be used in either PCASL or PASL approaches, since the hemodynamic information made available by quantifying ATT delays can improve quantification of CBF, or serve as useful hemodynamic measures in and of themselves (12,26)

Implementation details of both CASL and PASL labeling methods are described below.

CASL/PCASL Approaches

In CASL, a constant gradient is applied over the labeling period, and a constant RF pulse, tuned to resonate at the labeling plane, produces the flow-driven inversion as described above. In PCASL, the currently preferred implementation of CASL (17), the continuous RF is replaced by a long train of slice-selective RF pulses applied at the labeling plane, along with a train of gradient pulses that have a small but non-zero mean value. The mean value of both RF and gradient pulses over time are similar to those used in CASL, and the mechanism of inversion is the same. PCASL is preferred over CASL for two reasons. First, CASL produces significant saturation of brain tissue through magnetization transfer effects, leading to subtraction errors between label and control states. In addition, pulse sequence modifications that have been introduced to reduce these errors lead to decreased labeling efficiency. In PCASL, larger gradients are present during RF pulses, increasing the resonant offset of the pulses relative to brain tissue, and thereby decreasing magnetization transfer effects and increasing labeling efficiency. Second, CASL requires continuous application of RF power, which most current RF amplifiers cannot provide without modification, whereas PCASL is compatible with existing RF amplifiers.

Several variants of PCASL have been proposed, and whereas some variants can correct for potential artifacts and others can provide more information such as vascular territories, we currently recommend use of the basic implementation described here for robustness and simplicity and because there is sufficient experience in clinical use to support this recommendation.

The RF pulse spacing should be as short as possible. This directly affects the sensitivity of the labeling process to resonance offsets at the labeling plane, as well as labeling efficiency (27–29). A spacing of 1 ms from the center of one pulse to the center of the next is a good goal, but additional insensitivity to frequency offsets is gained with further reduction of the pulse spacing. For the labeling pulse, the slice-selective gradients should be ~10 mT/m with a mean gradient of ~1 mT/m, and the RF pulses should have a mean B_1 of ~1.5μT (17,27). The slice profile of the RF pulses should be sufficiently narrow to avoid labeling at the aliased labeling planes generated by the periodic pulses [see Dai et al. (17)]. In order for the pulses to remain in phase with the spins, the phase ϕ_n of the *n*th RF pulse should be $\phi_n = \gamma n\bar{G}TZ$, where γ is the gyromagnetic ratio, $\bar{G}$is the mean gradient, *T* is the RF pulse spacing, and *Z* is the distance from the isocenter of the gradients to the labeling plane (17). For the control condition, the phase of every other RF pulse should be shifted by π relative to the label condition, and the refocusing gradient lobes increased in amplitude such that the mean gradient is zero. In the literature, this gradient condition is referred to as an unbalanced control because the gradients in the label and control conditions are different (unbalanced). A balanced control is used in some implementations to facilitate vascular territory imaging, but has greater sensitivity to off-resonance effects, and is not preferred for basic PCASL (27).

The optimal label duration is determined by the relaxation time of the label (T_1), and also by the effect of the label duration on the repetition time (TR). The ASL signal increases with label duration, but with diminishing returns for label durations much longer than the T_1 of blood. Longer durations increase TR, and thereby decrease the number of averages obtained per unit time. Durations as long as 4 s may increase SNR and help preserve signal when ATT is unexpectedly long. However, long labeling durations increase signal dependence on tissue T_1 and may be unattainable due to power deposition and background suppression constraints. Because clinical experience with longer labeling times is less extensive, we recommend 1800 ms labeling duration in Table 1 as a current compromise between SNR increase

and disadvantages of greater power deposition, T_1 sensitivity, and limited clinical experience. (9,30).

Several methods have been used to choose the location of the labeling plane. In the ideal case, the labeling plane should be located in a region where the relevant feeding arteries are relatively straight and perpendicular to the labeling plane. This can be accomplished using an angiogram if one is available, and a fast angiogram that is sufficient for this purpose can be obtained in less than 1 min. However, the use of an angiogram for this purpose can add overall scan time and provides more opportunities for operator-related variability. A viable alternative is to use anatomical landmarks for selection of the labeling plane, and at least two approaches have been used successfully. One approach involves choosing a plane that is 85 mm inferior to the anterior commissure-posterior commissure (AC-PC) line (31). This method is appropriate for adults but is likely suboptimal for children. A second choice is to place the labeling plane just below the inferior border of the cerebellum to ensure labeling of the posterior cerebral circulation (32). It would be helpful if future ASL implementations allowed the user to easily control the location of the labeling plane for PCASL, perhaps through the graphical prescription interface of the scanner. There is not yet strong evidence that one of these methods is clearly superior to the other, and choosing an approach that integrates well with the local workflow is reasonable. Likewise, the choice of angiogram-based versus anatomical selection of the labeling plane should depend on the time constraints of the application and the consistency and expertise of the scanner operators.

When the RF pulses are not on-resonance at the labeling plane, inefficient labeling can result. It is therefore useful to avoid labeling in regions of strong susceptibility artifacts, such as air–bone interfaces. However, such failures are rare and are considered relatively easy to recognize with some experience, as they typically affect a single vascular territory and result in uniformly low signal throughout the territory, with no apparent compensatory redistribution of flow (Fig. 4). More subtle reductions in labeling efficiency may also occur due to alterations in B_0 or B_1 at the labeling location. There are currently several methods under investigation to characterize, prevent, or correct this artifact, including methods to shim or measure the fields at the labeling plane and correct for field offsets in the labeling process (28,29,33,34). However, these methods add complexity to the scanning process and have not yet been streamlined and tested for robustness in the clinical setting, and are therefore not recommended for general use at this time. Because gross labeling artifacts are relatively rare and can be recognized with experience, this potential problem is outweighed by the benefits of PCASL described above, and PCASL remains our clear recommendation as a first choice for ASL.

Pulsed ASL Approaches

In PASL, an RF pulse inverts a slab of tissue, including arteries, proximal to the area of interest. Many PASL labeling methods, and associated acronyms, have been introduced to produce this inversion, but overall, the methods are more similar than different. In publications we recommend identifying the ASL method first as PASL, and secondarily with the variant name in order to reduce confusion about the apparent wide variety of ASL methods. One difference that can be observed between PASL methods is in the labeling of spins that flow into the region of interest from the distal side. When whole brain coverage is specified, then the region distal to the imaging region is outside the head, and this distinction becomes irrelevant. For smaller imaging slabs, vessels entering from above the slab (mostly veins) may produce ASL signals. For flow-sensitive alternating inversion recovery (FAIR) (20) and its variants, inflow from above will produce a positive ASL signal. For echo planar imaging and signal targeting with alternating RF (EPISTAR) (13), inflow from above will produce a negative signal, and for proximal inversion with a control for off-resonance effects (PICORE) (25), pulsed star labeling of arterial regions (PULSAR) (35) and double inversions with proximal labeling of both tag and control images (DIPLOMA) (36), inflow from above produces no ASL signal. These labeling methods are all acceptable, but the user should be aware of the potential differences in the signal from inflowing distal spins. For efficient inversion, RF pulses should be insensitive to B_1 inhomogeneities, and the use of adiabatic inversion pulses (37,38) is therefore advocated. The total RF power during the label and control conditions should be equal to minimize magnetization transfer effects (39), a condition which is met by most implementations of PASL, including those referenced above. In addition, the slice profile of the slab-selective inversion pulse should be optimized to avoid overlap with the imaging volume (37,38). Saturation of the imaging volume just before and/or after the label and control pulses is recommended to minimize any residual label/control differences from magnetization transfer and/or slice profile effects, and also as an initial step in the background suppression process described below. The labeling inversion pulse should have been tested in a phantom, showing an inversion efficiency greater than 95%.

As mentioned above, a drawback of PASL is that it creates a bolus of labeled spins with an unknown and relatively short temporal width. It is possible to control

Table 1
Recommended Labeling Parameters

Parameter	Value
PCASL labeling duration	1800 ms
PCASL PLD: neonates	2000 ms
PCASL PLD: children	1500 ms
PCASL PLD: healthy subjects <70 y	1800 ms
PCASL PLD: healthy subjects >70 y	2000 ms
PCASL PLD: adult clinical patients	2000 ms
PCASL: average labeling gradient	1 mT/m
PCASL: slice-selective labeling gradient	10 mT/m
PCASL: average B_1	1.5 μT
PASL TI_1	800 ms
PASL TI	Use PCASL PLD (from above)
PASL labeling slab thickness	15–20 cm

the width of the labeling bolus by means of the QUIPSS-II modification (40), in which a slab-selective saturation pulse that matches the labeling slab is used to remove the tail end of the labeled bolus. This adaptation is necessary for quantification of CBF using PASL with a single delay time. However, for single delay time measurements PCASL is, in general, the preferred labeling method, as both SNR and repeatability are higher (41).

The labeling slab should have a thickness between 15 and 20 cm, with a gap to the imaging volume that is minimized subject to the constraint that the labeling pulse does not significantly perturb the magnetization in the imaging volume (typically a gap of 1–2 cm). For the purpose of generating a labeled bolus (and therefore an ASL signal) of maximum size, the thickness of the labeling slab should be as large as possible. However, three factors limit the optimal size of the labeling slab. First, for all PASL labeling methods other than FAIR, the width of the transition zone between inverted and uninverted blood at the edge of the labeled bolus is proportional to the thickness of the labeling slab (for FAIR, it is proportional to the thickness of the imaging slab). For large slab thickness, the transition zone becomes larger, requiring a larger gap between labeling and imaging slabs, which in turn increases arterial transit times and longer transit delays. Second, the RF transmit coil is limited in size, and the transmit B_1 falls off with distance from isocenter. For optimal quantitation of CBF, the labeled bolus should consist of completely inverted blood, and so the labeling slab should be limited to the region of relative homogeneity of the transmit RF fields. Finally, if the labeling bolus is beyond the homogeneous region of the transmit RF coil, not only will the tail end of the labeled bolus be incompletely inverted, but this partially inverted blood will take a long time to clear from the labeling slab, requiring a longer TR before the next labeling pulse and thus lowering time efficiency. Empirically, 15–20 cm has been found to be a good compromise between these factors.

One potential advantage of PASL over PCASL is lower RF power deposition, and this should be considered when the specific absorption rate is limiting. Up to 3T, specific absorption rate in PCASL has not been found to be a limiting factor across the range of patient sizes from infants (42) to adults (17).

Time Delay Between Labeling and Imaging

As noted in the Introduction, ASL methods employ a time delay between the application of the labeling pulse and image acquisition in order to allow for the labeled bolus to flow into the target tissue in the imaging region (Fig. 3). This time delay is used to allow labeled arterial water to reach the microcirculation and reduce the contribution of arterial signals to the perfusion image, which would otherwise appear as spots of apparent hyperperfusion. The delay also reduces the sensitivity of perfusion quantification to variations in transit time (9). The terminology that has developed to describe this delay is different for PCASL and PASL, which can be confusing, and is defined here. For PCASL, two time points define the timing of the labeling pulse train, the beginning, and the end, which are separated by the labeling duration of 1500–2000 ms (see above). The time between the end of this pulse train and image acquisition is referred to as the PLD. For PASL, the timing of the labeling pulse is characterized by a single time point, since the labeling pulse is nearly instantaneous (tens of milliseconds). The time from the application of this pulse to image acquisition is referred to as the inversion time (TI). Because PLD refers to the time at which the end of the labeled bolus leaves the labeling plane in PCASL, the analogous time in PASL is the time at which the end of the labeled bolus passes through the distal end of the labeling slab. In PASL, this time is generally unknown, as the temporal width of the labeled bolus in PASL is not controlled. With the QUIPSS II modification mentioned earlier, the bolus width is controlled and is referred to as TI_1. The PLD in PCASL is analogous to the quantity ($TI-TI_1$), as indicated in Fig. 3.

Single PLD/TI Methods

For CBF quantification using PCASL, the ideal case is that the PLD is set just longer than the longest value of ATT present in the subject. Under these conditions, the entire labeled bolus is delivered to the tissue prior to image acquisition, and the CBF measurement will be unbiased by incomplete delivery. However, because the ASL signal decays with time constant T_1 after labeling, it is too costly in terms of SNR to be extremely conservative in the choice of PLD such that PLD is guaranteed to be strictly longer than ATT under all circumstances. In healthy gray matter, ATT can vary between 500–1500 ms depending on the labeling location and the tissue location in the brain, but in cerebrovascular disease and in deep white matter, ATT can be 2000 ms or longer. The choice of PLD is therefore a compromise, such that SNR is acceptable, and that in the large majority of cases the ASL signal will accurately reflect CBF. However, it should be understood that areas of low ASL signal may reflect some combination of low CBF and unusually long ATT, and not specifically low CBF. In many cases, long ATT can be identified by the presence of intraluminal signal in the same vascular distribution due to spin label remaining in arteries. The range of expected ATT depends on age, and the PLD should be adjusted accordingly. Recommended values for PLD are given in Table 1, with a PLD of 2000 ms recommended for the clinical adult population, independent of age, given the potential for a wide variety of pathologies, which are often not known in advance of imaging.

Using PCASL with a single value of PLD, as described above, is a robust and straightforward means of obtaining reliable CBF images, and is therefore recommended as a standard clinical protocol. PASL with the QUIPSS II modification is analogous to PCASL in that it has a well defined labeled bolus duration, and allows for quantification of CBF using a single value of TI (40). However, this approach is only recommended when PCASL is unavailable, as the SNR of PASL is significantly lower. For PASL with QUIPSS II, TI_1 should be set to 800ms, and the TI set as shown in Table 1. Note that the recommended values of PLD for PCASL are the same as the TI for PASL. This effectively results in a PLD for PASL that

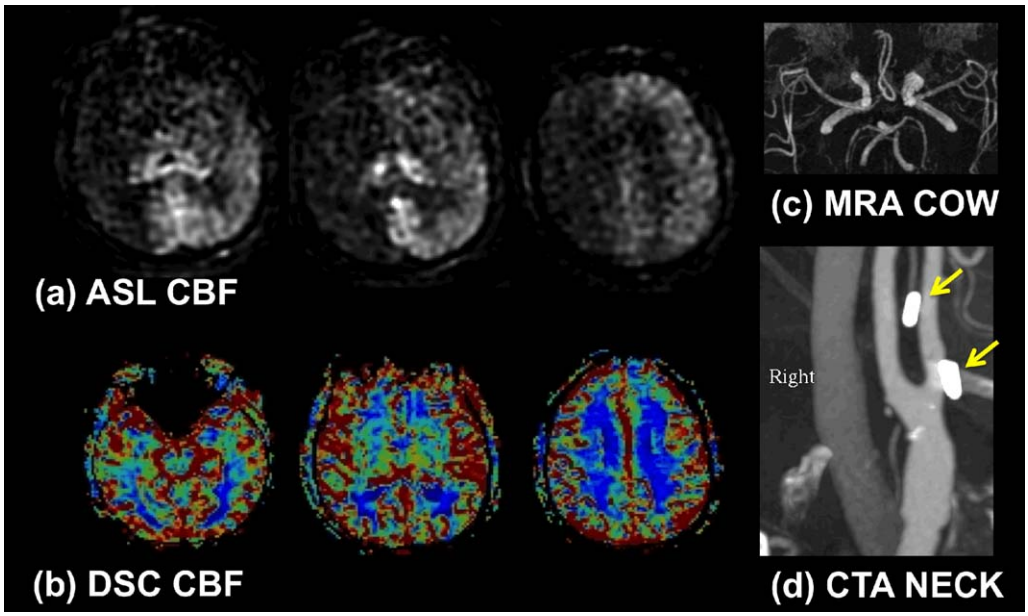

FIG. 4. **a:** Example of poor PCASL labeling within the right anterior circulation due to poor labeling of the right internal carotid artery. Note the loss of ASL signal confined to this territory without compensatory collateral flow. **b, c:** In this case, confirmation was obtained with a (b) normal dynamic susceptibility contrast CBF map and (c) normal MR angiogram of the circle of Willis. **d:** CT angiogram demonstrates surgical clips in the region of the right internal carotid artery (arrows), which may have been responsible for the poor labeling due to susceptibility effects.

is 800 ms shorter than that for PCASL. While this not ideal in that it increases the likelihood of incomplete delivery of labeled blood to the imaging region in PASL, it also increases SNR and was felt to be a necessary trade-off to compensate for the lower SNR inherent to PASL. Alternative approaches to recovering SNR, such as decreased spatial resolution, are also potentially effective, but have not been thoroughly tested in clinical practice.

Multiple PLD/TI Methods

The methods described above for single PLD/TI ASL imaging provide rapid and robust measures of CBF that are relatively insensitive to ATT. However, they do not provide measures of ATT, nor do they provide direct evidence that an abnormally long ATT may be introducing errors into the CBF measurement. Such effects might be particularly important in patients with steno-occlusive diseases. These effects have long been studied using PASL with multiple values of TI and fitting the data to estimate both CBF and ATT (43–46) but can also be studied with CASL or PCASL by varying PLD and labeling duration (30,32,47) or with more complex but efficient Hadamard time encoding strategies (48–50). While these multi-TI/PLD methods provide additional information, they are more complex, require more measurements and processing, and are therefore not recommended as a default ASL method at the present time. However, for those interested in the estimation of ATT or the most precise quantitation of CBF, we encourage the use of multi-TI/PLD methods. The ATT values estimated using this approach may themselves be of diagnostic utility, and the collection of ATT data on clinical populations will allow for more reliable optimization of PLD for single PLD imaging in the future, or may point to populations in which multi-TI/PLD imaging is especially useful.

Background Suppression

In gray matter, perfusion replaces ~1% of the brain water with in-flowing blood water every second. Therefore, a 2-s bolus of labeled blood in an ASL measurement can only perturb ~2% of the magnetization in a typical brain voxel. Considering the PLD and T_1 relaxation, the difference between label and control images is typically <1% of the relaxed brain signal. Unfortunately, subject motion, which is typically the dominant noise source in ASL, produces signal fluctuations (noise and/or artifacts) that are proportional to the signal intensity in the unsubtracted images. Therefore, if it is possible to decrease the signal intensity of the unsubtracted images without a proportional decrease in the ASL difference signal, the overall SNR of the ASL measurement can be improved substantially (51,52). Such a decrease of the signal intensity unmodulated by labeling can be accomplished using a combination of spatially selective saturation and inversion pulses. This technique is usually referred to as background suppression (BS). ASL MRI scans incorporating background suppression have markedly improved temporal SNR, which is of particular value in clinical ASL where scan times must be as short as possible and inferences are being made on perfusion data from a single scan (53,54).

Details about the implementation and optimization of BS for ASL can be found in (17,55,56), but briefly: an initial saturation pulse selective to the imaging region,

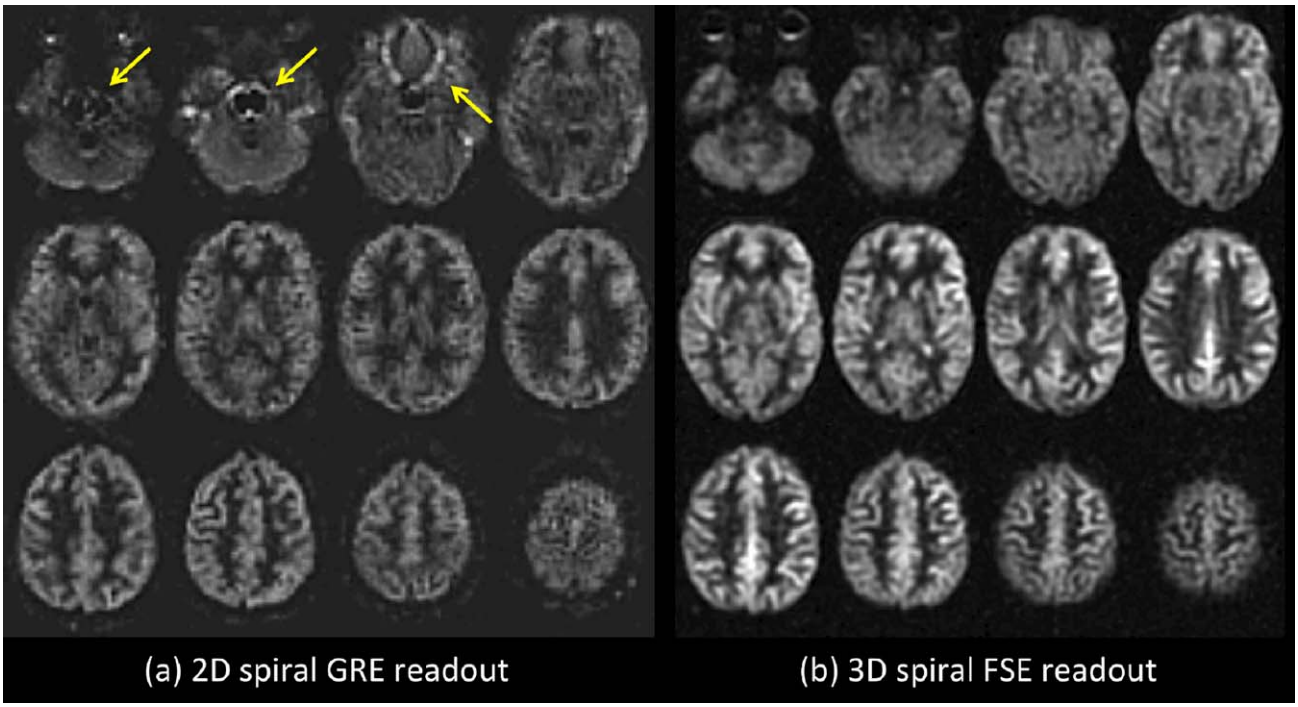

FIG. 5. 2D (**a**) versus 3D (**b**) readout ASL imaging in a normal subject. Both sets of images were acquired with ~5 min of imaging at 3T with PCASL labeling (label duration, 1.5 s; PLD, 2 s). The 2D readout method was a single-shot gradient echo spiral. The 3D readout was a segmented stack of spirals fast spin echo. Arrows indicate the artifacts associated with the 2D single-shot method in regions of high susceptibility. Parallel imaging approaches could be used to improve such artifacts associated with single-shot gradient echo imaging.

followed by carefully timed inversion pulses, results in the longitudinal magnetization of static tissue passing near or through zero at the time of image acquisition. The blood that is to be labeled by the labeling pulses does not experience the initial saturation, but does experience the inversion pulses. For perfect inversion pulses, each inversion changes the sign of the ASL label/control magnetization difference, but nominally does not affect the magnitude of this difference. Thus, the ASL signal is preserved, while the static tissue signal is nearly eliminated.

Two important features of BS should be emphasized. First, there is a trade-off in the number of inversion pulses used for BS. The larger the number of inversion pulses, the more accurately static tissue can be suppressed over a wide range of tissue T_1 values. The trade-off is that each inversion pulse reduces the ASL label/control difference signal. The efficiency of the inversion pulses is high but not perfect, and is typically ~95%, so each inversion pulse reduces the ASL signal by ~5%. In each implementation, this trade-off should be evaluated, and the efficiency of the inversion pulse measured in vivo or appropriate phantoms (56), so that this source of signal loss can be accounted for in the calculation of CBF. Generally, two pulses can be considered a good trade-off. We do not, however, recommend efficiency measurement on each subject, as the added time required does not seem justified by any observations of large intersubject differences. A second key feature is that BS only nulls the magnetization of static tissue at one point in time, after which the magnetization of static tissue continues to grow toward the equilibrium state by relaxation. For imaging methods that employ a single excitation per TR, such as the segmented 3D approaches describe below, BS can be highly effective, as the null point of the magnetization can be timed to coincide with the excitation pulse. For methods that require multiple excitations per TR, such as multislice single-shot two-dimensional (2D) methods, BS can be optimal for one slice, but is progressively less efficient for other slices. This difference in BS efficiency can interact strongly with the choice of imaging methods for ASL, as discussed below.

Readout Approaches

For the readout module of ASL, segmented 3D sequences are the preferred methodology because they use a single excitation per TR, which is optimal for BS, and because they can be made SNR efficient and relatively insensitive to off-resonance effects. It is anticipated that single-shot 3D readout may be the preferred option in the future, but these methods are not yet sufficiently well tested to recommend for general use at this time. Multislice single-shot 2D echo-planar imaging (EPI) or spiral readout should be considered a viable alternative to segmented 3D sequences, because they are available on all systems and are insensitive to image artifacts from motion. However, 2D imaging results in poor BS for most slices, as well as longer scan time. Examples of ASL with 2D and 3D readouts are shown in Fig. 5, and more detailed comparisons

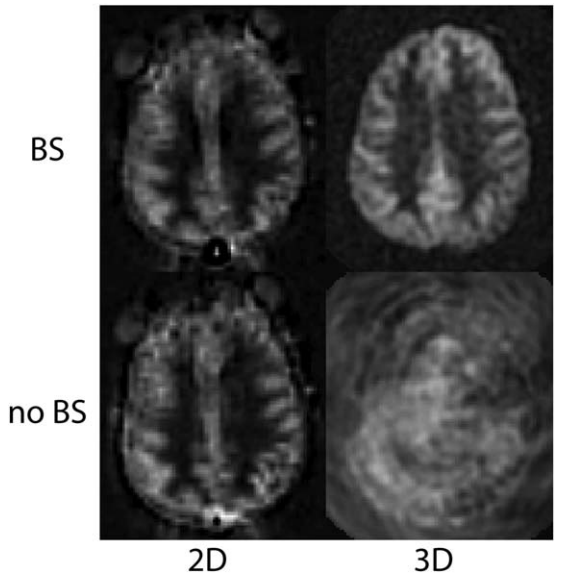

FIG. 6. PCASL images acquired using 2D single-shot and 3D segmented spiral readouts, with and without BS.

between these methods in ASL can be found in Vidorreta et al. (57) and Nielsen and Hernandez-Garcia (58).

Segmented 3D Readout

As a default readout, 3D segmented methods such as 3D multiecho (RARE) stack of spirals (52,57) or 3D GRASE (59–61) are recommended. These methods provide nearly optimal SNR for measurement of the magnetization prepared by the ASL pulses, and they are relatively insensitive to field inhomogeneity. They strike a balance between the T2* insensitivity of pure RARE methods, and the time efficiency of pure EPI or spiral acquisitions, enjoying most of the benefits of both. Compared with 2D multislice readouts, these methods allow for significantly better BS. BS is only optimal at one point in time, and because segmented 3D readouts only require one excitation per TR period, the excitation can be timed to provide a very high degree of BS. BS parameters should be optimized for minimal static tissue signal, and a complex difference between label and control images should be calculated to form the ASL signal, as a difference between magnitude reconstructed images that are near zero will generate sign ambiguities. Note that the use of BS for segmented 3D acquisitions is critical for ASL, as shown in Fig. 6. Segmented methods require data consistency between excitations, and without BS, the motion-related artifacts will generally dominate the ASL signal (Fig. 6, bottom right). For 3D readouts, the time within each TR that is allocated to image acquisition is generally shorter than that of multiple 2D slices (unless the number of slices is very small), allowing for more efficient use of time (ie, shorter TR, or longer labeling time per TR). 3D RARE stack of spirals and 3D GRASE perform similarly (57), and we recommend whichever of these two is better optimized on a particular system. We note that the stack of spiral acquisition provides natural oversampling at the center of k-space, which can improve motion insensitivity, but also has the potential for in-plane blurring due to resonance offsets. In contrast, GRASE typically does not oversample k-space, and resonance offsets in 3D GRASE result in in-plane distortion rather than blurring. For this multishot acquisition, label and control conditions for a given shot should be acquired sequentially in time (ie, the label/control modulation should be the inner-most loop) to achieve the most accurate label/control subtraction. The user should also be aware that T_2-related signal modulation across echoes can result in through-plane blurring. If the image reconstruction software is vendor-supplied, we recommend inquiring as to what methods are used to correct for image blurring and/or distortion so that the images can be interpreted accordingly. The methods and parameters used for these corrections should be described in manuscripts that report ASL data, as they can have a significant impact on the comparison of data between sites. See Table 2 for recommended imaging parameters.

Single-Shot 2D Readout

As a second choice, 2D single-shot imaging methods can be used effectively for ASL. EPI and spiral methods have been used extensively, while single-shot RARE and balanced SSFP are also viable, but are less common and much less thoroughly tested for ASL. EPI and spiral have similar performance to one another for ASL, again with small differences. Spirals allow for shorter echo time (TE) to reduce T2/T2* weighting but suffer from off-resonance–related blurring. EPI has longer minimum TE but demonstrates distortion rather than blurring in the presence of resonance offsets. As for 3D imaging, we recommend whichever of the two methods is better optimized on a particular system. Generally, an ascending slice order is recommended for single-shot 2D readouts. One advantage of single-shot imaging methods is that they are immune to motion artifacts from the

Table 2
Recommended Imaging Parameters

Parameter	Value
Spatial resolution	3–4 mm in-plane, 4–8 mm through-plane
3D RARE stack of spiral or 3D GRASE	4–15 ms readouts, turbo-factor of 8–12, echo train of up to 300 ms
2D EPI or spiral	Single shot, minimum echo time
Scan time	4 min for acute cases, 2 min with lower spatial resolution
Field strength	Use 3T when available; for 1.5T, use lower spatial resolution
Vascular crushing gradients	Not recommended under most circumstances; when applicable, use VENC = 4 cm/s in the Z-direction

inconsistency between excitations that can affect multi-shot methods. However, this sensitivity in 3D segmented imaging is minimized by the use of efficient BS, as shown in Fig. 6. For 2D imaging, BS will only be optimal for one or a few slices. Although this is generally a drawback, the residual static tissue signal can be useful in two ways. First, magnitude image reconstruction can be used, which can be simpler than complex reconstruction and coil combination; second, the residual signal can be used for image registration prior to label-control subtraction. While the effects of BS in 2D single-shot imaging is much less dramatic than in 3D imaging (Fig. 6), significant decreases in signal fluctuations are seen, especially with significant patient motion, and the use of BS is recommended. See Table 2 for further recommended imaging parameters.

Parallel Acceleration

Parallel imaging can be used to reduce imaging time by undersampling k-space and using the spatial information from multichannel coils to reconstruct undersampled data. This acceleration can come at a cost in SNR, and as ASL is significantly SNR limited, parallel acceleration should be used judiciously. We recommend the use of moderate acceleration factors of 2–3 for the following purposes: to reduce the echo train length for RARE-based methods such as 3D RARE stack of spirals or 3D GRASE, when the echo train would otherwise be significantly longer than T_2; or to reduce the echo time for 2D gradient echo EPI (this is not necessary for 2D spiral).

Vascular Crushing Gradients

By means of the insertion of vascular crushing gradients directly after the excitation pulse or a motion-sensitized T2-preparation module, vascular artifacts can be reduced by dephasing signal from label still present in larger arteries at the time of imaging. Elimination of this signal is based on the velocity of the spins in the direction of the gradients (frequently only the feet–head direction). Because of the additional gradients or the use of a T2-preparation module, the effective TE will be prolonged when using vascular crushing, thereby introducing T2 (or T2*) contrast into the ASL-image and a reduction in SNR. This should be taken into account in the calculation of CBF (62).

As a default implementation, we discourage the use of vascular crushing gradients, given that they may remove important clinical information, such as the presence of delayed flow and arteriovenous shunting. For single PLD imaging, the PLD is chosen so that it will be longer than ATT for the majority of cases. When this condition is true, the labeled bolus will be delivered to target tissues prior to imaging, and little if any labeled blood will be in larger arteries at the time of imaging. In this case, the effects of vascular crushing gradients on the ASL image will be minimal. However, when regions exist with ATT>PLD, bright vascular signals will appear in the ASL image, and these signals would be removed using vascular crushing gradients. For some applications, such as in the setting of collateral flow (63), the presence of bright vascular signal may be a useful indicator that regions with long ATT are present and that quantitative CBF values distal to these regions may be in error; this information may itself be of diagnostic value. In arteriovenous malformations, the identification of ASL signals in veins may also be clinically useful (64,65) (Fig. 7).

We encourage the implementation of vascular crushing gradients as a user-controlled option, as they will likely be useful under some circumstances, but not others. For applications such as in tumors, bright intravascular signals may obscure more subtle underlying perfusion-related signals of interest, and vascular crushing gradients may be desirable. When time is available, two ASL scans with and without vascular crushing gradients may provide the most useful information. These choices are related to the manner in which ASL will ultimately be used in the clinical setting, which is not yet well established. We encourage users to become familiar with the effects outlined above, and to experiment with this option.

For multi-PLD/TI imaging, ATT can be estimated in addition to CBF, as discussed above. Without vascular crushing gradients, the measured ATT will indicate the time at which the labeled bolus arrives in the voxel, while with vascular crushing gradients the measures ATT will reflect the arrival time in the microvasculature. These different ATTs may be of interest in different applications. Without vascular crushing gradients, care should be taken to include in-flow effects in the model, otherwise the calculated CBF may not be correct.

An additional note on the use of vascular crushing gradients is that when perfusion imaging is performed as part of a group analysis, vascular artifacts can complicate the analysis due to the presence of hyperintense spots at irregular locations (corresponding to large arteries), and the use of vascular crushing gradients could be considered in this setting.

Vascular crushing is characterized by the VENC, or the velocity at which flow induces a phase shift of 180°. Roughly speaking, spins are dephased above VENC, and remain visible below VENC. Very high VENC allows large arterial signal to remain, while very low VENC results in prolonged ATT and low SNR. When used, we recommend vascular crushing in the feet–head direction with a VENC of 4 cm/s as a good trade-off.

Postprocessing Methods

In routine clinical practice, visualization of the ASL difference (label–control) images is most useful, as most disorders of perfusion result in easily visualizable focal changes. However, we recommend that additional CBF imaging in quantitative units also be provided, given that some disorders do cause global changes (such as hypercapnia or hypoxic ischemic injury).

Quantification of CBF

One of the most attractive features of ASL is its ability to quantify perfusion, an important indicator of tissue health as well as neuronal activity. For quantification of CBF from single PLD/TI ASL data, a relatively basic model is proposed. The major assumptions of this model are:

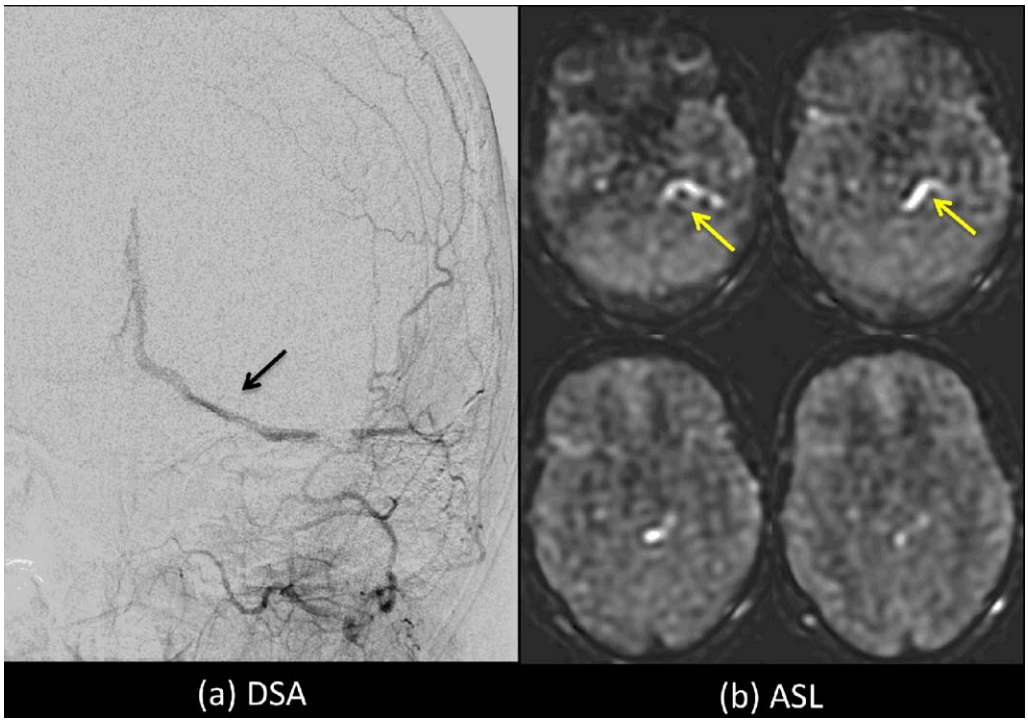

FIG. 7. **a:** Digital subtraction angiogram (DSA), demonstrating arteriovenous shunting in a patient with a dural AV fistula (black arrow). **b:** Intraluminal ASL signal within veins (yellow arrows). Use of vascular crushing may suppress such information, limiting the clinical value of ASL in this type of case.

1. The entire labeled bolus is delivered to the target tissue. This is the case when PLD > ATT for PCASL, or (TI-TI1) > ATT for QUIPSS II PASL.
2. There is no outflow of labeled blood water. Because the tissue water pool is much larger than the blood water pool, and water exchange between blood and tissue is rapid, this is generally a valid assumption (66).
3. The relaxation of the labeled spins are governed by blood T_1. While this assumption is not likely to be strictly true, the errors introduced by this assumption, which are related to the difference in T_1 between blood and tissue, are typically relatively small.

Under these assumptions, CBF in each voxel can be calculated for PCASL using (43)

$$\mathrm{CBF} = \frac{6000 \cdot \lambda \cdot (\mathrm{SI_{control}} - \mathrm{SI_{label}}) \cdot e^{\frac{\mathrm{PLD}}{T_{1,\ \mathrm{blood}}}}}{2 \cdot \alpha \cdot T_{1,\mathrm{blood}} \cdot \mathrm{SI_{PD}} \cdot (1\text{-}e^{-\frac{\tau}{T_{1,\mathrm{blood}}}})} \ [\mathrm{ml/100\ g/min}] \quad [1]$$

and for QUIPSS II PASL using (40)

$$\mathrm{CBF} = \frac{6000 \cdot \lambda \cdot (\mathrm{SI_{control}} - \mathrm{SI_{label}}) \cdot e^{\frac{\mathrm{TI}}{T_{1,\ \mathrm{blood}}}}}{2 \cdot \alpha \cdot \mathrm{TI_1} \cdot \mathrm{SI_{PD}}} \ [\mathrm{ml/100\ g/min}] \quad [2]$$

where λ is the brain/blood partition coefficient in mL/g, $SI_{control}$ and SI_{label} are the time-averaged signal intensities in the control and label images, respectively, $T_{1,blood}$ is the longitudinal relaxation time of blood in seconds, α is the labeling efficiency, SI_{PD} is the signal intensity of a proton density-weighted image, and τ is the label duration. PLD, TI, and TI_1 are as defined above. The factor of 6000 converts the units from mL/g/s to mL/(100 g)/min, which is customary in the physiological literature. Note that for 2D multislice imaging, the value of TI in these expressions should be adjusted for each slice to take into account the time delay between slice acquisitions. See Table 3 for a summary of parameters for use in CBF quantification. Single TI PASL without the QUIPSS II modification cannot be reliably converted into CBF.

To scale the signal intensities of the subtracted ASL images to absolute CBF units, the signal intensity of fully relaxed blood spins is needed. Although several approaches can yield estimates of this value, we recommend using a separately acquired proton density (PD) image (represented by SI_{PD} in the above equations) to obtain this scaling factor on a voxel-by-voxel basis. The factor λ scales the signal intensity of tissue to that of blood. In principle, λ should be an image because tissue

Table 3
Values To Be Used in Quantification of ASL Data

Parameter	Value
λ (blood–brain partition coefficient)	0.9 mL/g (74)
$T_{1,blood}$ at 3.0T	1650 ms (10)
$T_{1,blood}$ at 1.5T	1350 ms (75)
α (labeling efficiency) for PCASL	0.85 (17)
α (labeling efficiency) for PASL	0.98 (19)

water density differs in different tissue types, but often a brain average value is used. Strategies to measure λ (67) or to quantify CBF without using λ (68,69) have been proposed but are not in widespread use. Quantification errors associated with the constant λ assumption are expected to be <10%. Here we recommend the use of a brain-averaged λ, at least until greater optimization and clinical evaluation of alternative strategies has been performed. The use of a PD image for this scaling serves two additional important functions. By dividing by this image, signal variations caused by RF coil inhomogeneity, as well as differences in transverse relaxation, are largely corrected as well. The PD image should have an identical readout module as the ASL label and control images, with a long TR to provide proton density weighting. If TR is <5 s, the PD image should be multiplied by the factor $\left(1/(1-e^{-TR/T_{1,tissue}})\right)$, where $T_{1,tissue}$ is the assumed T_1 of gray matter, in order to compensate for T_1 relaxation. Using a reduced TR and T_1 correction may potentially reduce errors associated with a brain-averaged λ (34,70). No labeling or BS should be applied for this scan. Care should be taken that the absolute scaling between the signal intensities in this acquisition and the ASL scans is known. Note that since this PD image goes in the denominator of the equation, it is important that its SNR is high and that it is well-coregistered with the images in the numerator, otherwise its noise contribution can be greatly amplified. A good way of ensuring this is to apply a motion correction scheme and a smoothing filter (typically a Gaussian filter of 5–8 mm diameter) to the PD image.

This model is simplified, but is recommended for its robustness and simplicity, and because more complete models require additional information that involves more scan time, and often only reduces systematic errors at the cost of SNR. Types of additional information include ATT, water exchange rates and times between blood and tissue, tissue T_1 values, and tissue segmentation. Ongoing active research aims to more fully understand the range and effects of these parameters, but the complexity, uncertainty, and additional noise associated with correcting for these factors was deemed to be counterproductive as a default protocol at this stage of adoption of clinical ASL.

Estimation of parameters from multi-PLD/TI ASL data is also an area of active research and depends in detail on the acquisition parameters and the model used (71). It is beyond the scope of this article, but we encourage the user to become familiar with this area of work, as it may be useful in the interpretation of clinical ASL images.

ASL in the Clinical Setting

Scan Time

Because the ASL signal is small, ASL relies on averaging to achieve sufficient SNR. Increasing the number of averages increases SNR, mitigates the effects of motion artifacts, and also provides more opportunities for data filtering. When using the default parameters described here, a total scan time of ~4 min results in good image quality in cooperative subjects. For fast imaging in an acute setting, scan times as low as 2 min may provide interpretable data, and in these cases we recommend that spatial resolution should be lowered to compensate for the SNR loss.

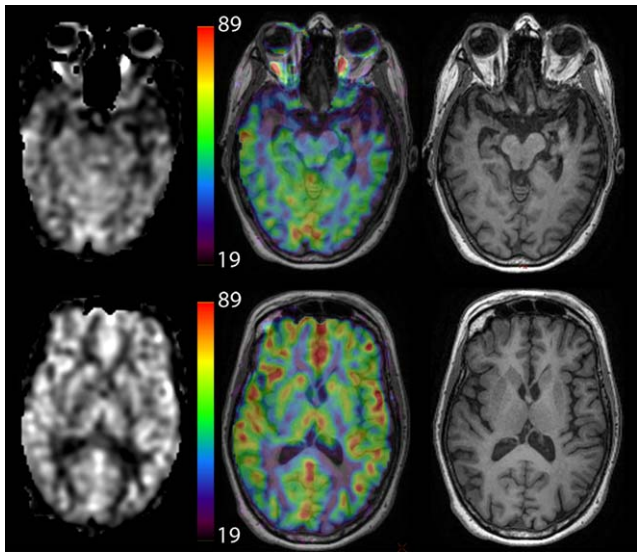

FIG. 8. Example of different methods of displaying CBF information in a patient with semantic dementia (note the low CBF in the left temporal lobe). The images on the left are CBF maps, whereas the center images show CBF maps using a color map overlaid on high-resolution T_1-weighted images, which are shown separately on the right. The color scale is in mL/min/100 g. Color CBF maps may be displayed without anatomical underlay as well.

Visualization

One of the key strengths of ASL is that it can produce absolute measures of CBF. We recommend viewing the resulting CBF images in either grayscale or color, with a quantitative scale bar next to the images to indicate CBF values (Fig. 8). The use of color can improve the ability to read quantitative CBF values from the scale bar but can also lead to false apparent thresholds, and the user should be aware of this potential pitfall.

Detection of White Matter Perfusion

Detection and interpretation of perfusion abnormalities in the white matter remains challenging due to low SNR caused by the lower blood flow and prolonged ATT of white matter compared to grey matter. Furthermore, the white matter ASL signal can easily be overwhelmed by gray matter signal due to blurring in either in-plane or through-plane directions (72). The sensitivity for detection of white matter perfusion deficits should therefore be considered to be too small for general clinical use, though pathologies that exhibit increased perfusion (such as some tumors), may be detectable.

Quality Assurance

For evaluating the quality of ASL MRI images in clinical practice, we advise the following checks:

1. **For PCASL scans, look for areas of low labeling efficiency**. First, identify which arteries should have been labeled. Typically, this will include internal and external carotid arteries, and vertebral arteries. If an angiogram is available, this can be used to verify the list of labeled arteries. Checking the circle of Willis anatomy may also be of use in matching vascular territories to labeled arteries. When the labeling efficiency is low in an artery, the entire flow territory of that artery will demonstrate a low calculated CBF. When a low CBF area is seen that matches an entire vascular territory, with no apparent compensation from other arteries, a labeling failure should be considered, though this does not preclude the possibility of truly low CBF conditions, or abnormally long ATT. Labeling failures can be caused by tortuous vessels or resonance offsets in the labeling plane. The former may be addressed by adjusting the location of the labeling plane, in which case an additional angiogram would be helpful. The latter is commonly caused by dental work, and may be suggested by signal dropouts around the teeth in other images from this patient. Methods to address resonance offset related labeling problems in PCASL are discussed above.
2. **Note the overall gray matter CBF value**. Absolute CBF values obtained in gray matter can vary significantly, even among healthy young adults, due to natural intersubject and intrasubject variations. In addition, average numbers are sensitive to partial volume effects and the methods used for isolating gray matter signal. As a general rule, gray matter CBF values from 40-100 mL/min/100 mL can be normal. When the overall gray matter CBF value is inconsistent with the expected values for the patient population, consider the possibility that there is a global reduction in labeling efficiency, or that the PD scan used for normalization was incorrectly acquired or scaled. Clear contrast between gray and white matter should be present, and if not, may signify either poor labeling or motion artifacts.
3. **Check for motion artifacts**. As a subtractive technique, ASL is motion sensitive, though this sensitivity is mitigated by BS as discussed above. The presence of signal outside of the brain, frequently recognizable as signal from layers of skin or fat is a clear indication of significant subject motion. When possible, it may be useful to check individual label/control difference images before averaging to see whether artifacts arise from only a minority of these difference images. If so, these images can be excluded from the CBF calculation. In addition, motion correction by means of automated image registration algorithms can be performed, though these may not be effective when BS is very efficient, or when applied to the label/control difference images, as the individual image SNR in these cases is low. When BS is not used or is incomplete, image registration is likely to be more effective, but BS is nevertheless recommended as a primary means of reducing physiological noise and motion artifacts. In the ideal case, prospective motion correction methods can be used when available to reduce motion artifacts during acquisition (73), and some of these methods are compatible with background suppression.
4. **Look for intravascular artifacts**. Hyperintense spots and serpiginous regions often represent intravascular signal. When observed, it is advisable to verify that the PLD was appropriate for the patient (see Table 1), as a low PLD will naturally generate ASL signals in larger arteries. Intra-arterial signal with a correct PLD suggests that delivery of labeled blood to tissue is delayed, through slow flow and/or circuitous or collateral routes of circulation. Intravenous ASL signal suggests that an arteriovenous shunt is present. Note that CBF calculations over whole brain or large regions of interest may still be valid in the presence of intravascular artifact as long as flow crushing gradients were not used.
5. **Check the borderzone (watershed) regions**. The borderzone or watershed areas are at the more distal portions of each vascular territory, and will naturally have a longer ATT than other portions of the territory. Note that it is possible for low ASL signal in these regions to represent long ATT rather than low CBF, and an additional scan with longer PLD may help to distinguish between these two possibilities. An example of this effect is shown in Fig. 9.

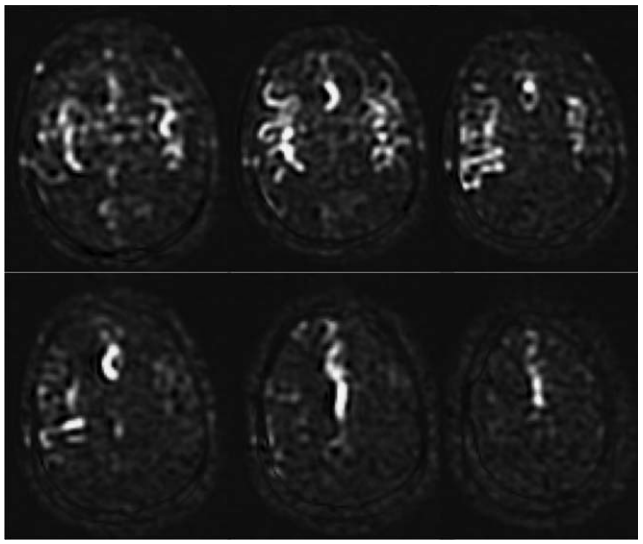

FIG. 9. Borderzone sign. These ASL subtraction images are from an 85-year-old man with dense left hemiparesis, acquired using PCASL with a labeling time of 1500 ms and a PLD of 1500 ms. Only the proximal portions of the arterial tree are present, indicating that the PLD was not long enough for the labeled spins to have reached the tissue, and that the ATT was prolonged bilaterally in this elderly patient. Although longer PLD should improve the visualization of parenchymal CBF, it is not uncommon to see such a finding, known as the borderzone sign, in elderly patients with extremely delayed arrival times.

SUMMARY

The guidelines described in this recommendation paper are intended to help provide clinicians with ASL images

of sufficient quality and SNR to provide diagnostic utility. As a default protocol, we have recommended PCASL labeling, BS, a segmented 3D RARE-based readout, and simple but quantitative data processing, and have tabulated recommended parameters. Although these recommendations are intended to promote uniformity and thereby comparability of ASL data across scanners and sites, experimentation with parameters and other ASL methods is encouraged when appropriate. Note that these recommendations are made as of the date of this publication, and will likely be superseded in the future, as more clinical data are collected and analyzed, and as current and future technical innovations undergo clinical translation.

ACKNOWLEDGMENTS

We thank the International Society for Magnetic Resonance in Medicine and the European Union COST agency (through COST Action BM1103) for sponsorship of their respective workshops in October 2012, at which the foundations of this consensus statement were formed. DCA is an inventor on patents related to PCASL and receives royalties on these inventions from GE Healthcare and Philips Healthcare through his current institution. His conflict related to PCASL was disclosed to other authors during discussions and guideline decisions.

REFERENCES

1. Bokkers RP, Bremmer JP, van Berckel BN, Lammertsma AA, Hendrikse J, Pluim JP, Kappelle LJ, Boellaard R, Klijn CJ. Arterial spin labeling perfusion MRI at multiple delay times: a correlative study with H(2)(15)O positron emission tomography in patients with symptomatic carotid artery occlusion. J Cereb Blood Flow Metab 2010;30:222–229.
2. Xu G, Rowley HA, Wu G, Alsop DC, Shankaranarayanan A, Dowling M, Christian BT, Oakes TR, Johnson SC. Reliability and precision of pseudo-continuous arterial spin labeling perfusion MRI on 3.0 T and comparison with 15O-water PET in elderly subjects at risk for Alzheimer's disease. NMR Biomed 2010;23:286–293.
3. Gevers S, van Osch MJ, Bokkers RP, Kies DA, Teeuwisse WM, Majoie CB, Hendrikse J, Nederveen AJ. Intra- and multicenter reproducibility of pulsed, continuous and pseudo-continuous arterial spin labeling methods for measuring cerebral perfusion. J Cereb Blood Flow Metab 2011;31:1706–1715.
4. Petersen ET, Mouridsen K, Golay X. The QUASAR reproducibility study, part II: results from a multi-center arterial spin labeling test-retest study. NeuroImage 2010;49:104–113.
5. Detre JA, Rao H, Wang DJ, Chen YF, Wang Z. Applications of arterial spin labeled MRI in the brain. J Magn Reson Imaging 2012;35:1026–1037.
6. Hendrikse J, Petersen ET, Golay X. Vascular disorders: insights from arterial spin labeling. Neuroimaging Clin N Am 2012;22:259–269, x–xi.
7. Detre JA, Leigh JS, Williams DS, Koretsky AP. Perfusion imaging. Magn Reson Med 1992;23:37–45.
8. Williams DS, Detre JA, Leigh JS, Koretsky AP. Magnetic resonance imaging of perfusion using spin inversion of arterial water. Proc Natl Acad Sci U S A 1992;89:212–216.
9. Alsop DC, Detre JA. Reduced transit-time sensitivity in noninvasive magnetic resonance imaging of human cerebral blood flow. J Cereb Blood Flow Metab 1996;16:1236–1249.
10. Lu H, Clingman C, Golay X, van Zijl PC. Determining the longitudinal relaxation time (T1) of blood at 3.0 Tesla. Magn Reson Med 2004; 52:679–682.
11. Zhang X, Petersen ET, Ghariq E, De Vis JB, Webb AG, Teeuwisse WM, Hendrikse J, van Osch MJ. In vivo blood T(1) measurements at 1.5 T, 3 T, and 7 T. Magn Reson Med 2013;70:1082–1086.
12. Bokkers RP, van der Worp HB, Mali WP, Hendrikse J. Noninvasive MR imaging of cerebral perfusion in patients with a carotid artery stenosis. Neurology 2009;73:869–875.
13. Wang J, Alsop DC, Li L, Listerud J, Gonzalez-At JB, Schnall MD, Detre JA. Comparison of quantitative perfusion imaging using arterial spin labeling at 1.5 and 4.0 Tesla. Magn Reson Med 2002;48:242–254.
14. Pruessmann KP, Weiger M, Scheidegger MB, Boesiger P. SENSE: sensitivity encoding for fast MRI. Magn Reson Med 1999;42:952–962.
15. Griswold MA, Jakob PM, Heidemann RM, Nittka M, Jellus V, Wang J, Kiefer B, Haase A. Generalized autocalibrating partially parallel acquisitions (GRAPPA). Magn Reson Med 2002;47:1202–1210.
16. Wang Z, Wang J, Detre JA. Improved data reconstruction method for GRAPPA. Magn Reson Med 2005;54:738–742.
17. Dai W, Garcia D, de Bazelaire C, Alsop DC. Continuous flow-driven inversion for arterial spin labeling using pulsed radio frequency and gradient fields. Magn Reson Med 2008;60:1488–1497.
18. Kwong KK, Chesler DA, Weisskoff RM, Donahue KM, Davis TL, Ostergaard L, Campbell TA, Rosen BR. MR perfusion studies with T1-weighted echo planar imaging. Magn Reson Med 1995;34:878–887.
19. Wong EC, Buxton RB, Frank LR. A theoretical and experimental comparison of continuous and pulsed arterial spin labeling techniques for quantitative perfusion imaging. Magn Reson Med 1998;40:348–355.
20. Kim SG. Quantification of relative cerebral blood flow change by flow-sensitive alternating inversion recovery (FAIR) technique: application to functional mapping. Magn Reson Med 1995;34:293–301.
21. Wong EC, Cronin M, Wu WC, Inglis B, Frank LR, Liu TT. Velocity-selective arterial spin labeling. Magn Reson Med 2006;55:1334–1341.
22. Detre JA, Zhang W, Roberts DA, Silva AC, Williams DS, Grandis DJ, Koretsky AP, Leigh JS. Tissue specific perfusion imaging using arterial spin labeling. NMR Biomed 1994;7:75–82.
23. Alsop DC, Detre JA. Multisection cerebral blood flow MR imaging with continuous arterial spin labeling. Radiology 1998;208:410–416.
24. Edelman RR, Chen Q. EPISTAR MRI: multislice mapping of cerebral blood flow. Magn Reson Med 1998;40:800–805.
25. Wong EC, Buxton RB, Frank LR. Implementation of quantitative perfusion imaging techniques for functional brain mapping using pulsed arterial spin labeling. NMR Biomed 1997;10:237–249.
26. Macintosh BJ, Marquardt L, Schulz UG, Jezzard P, Rothwell PM. Hemodynamic alterations in vertebrobasilar large artery disease assessed by arterial spin-labeling MR imaging. AJNR Am J Neuroradiol 2012;33:1939–1944.
27. Wu WC, Fernandez-Seara M, Detre JA, Wehrli FW, Wang J. A theoretical and experimental investigation of the tagging efficiency of pseudocontinuous arterial spin labeling. Magn Reson Med 2007;58:1020–1027.
28. Jahanian H, Noll DC, Hernandez-Garcia L. B0 field inhomogeneity considerations in pseudo-continuous arterial spin labeling (pCASL): effects on tagging efficiency and correction strategy. NMR Biomed 2011;24:1202–1209.
29. Shin DD, Liu TT, Wong EC, Shankaranarayanan A, Jung Y. Pseudo-continuous arterial spin labeling with optimized tagging efficiency. Magn Reson Med 2012;68:1135–1144.
30. Gonzalez-At JB, Alsop DC, Detre JA. Cerebral perfusion and arterial transit time changes during task activation determined with continuous arterial spin labeling. Magn Reson Med 2000;43:739–746.
31. Aslan S, Xu F, Wang PL, Uh J, Yezhuvath US, van Osch M, Lu H. Estimation of labeling efficiency in pseudocontinuous arterial spin labeling. Magn Reson Med 2010;63:765–771.
32. Dai W, Robson PM, Shankaranarayanan A, Alsop DC. Reduced resolution transit delay prescan for quantitative continuous arterial spin labeling perfusion imaging. Magn Reson Med 2012;67:1252–1265.
33. Luh WM, Talagala SL, Li TQ, Bandettini PA. Pseudo-continuous arterial spin labeling at 7 T for human brain: estimation and correction for off-resonance effects using a Prescan. Magn Reson Med 2013;69: 402–410.
34. Jung Y, Wong EC, Liu TT. Multiphase pseudocontinuous arterial spin labeling (MP-PCASL) for robust quantification of cerebral blood flow. Magn Reson Med 2010;64:799–810.
35. Golay X, Petersen ET, Hui F. Pulsed star labeling of arterial regions (PULSAR): a robust regional perfusion technique for high field imaging. Magn Reson Med 2005;53:15–21.
36. Jahng GH, Zhu XP, Matson GB, Weiner MW, Schuff N. Improved perfusion-weighted MRI by a novel double inversion with proximal labeling of both tagged and control acquisitions. Magn Reson Med 2003;49:307–314.

37. Frank LR, Wong EC, Buxton RB. Slice profile effects in adiabatic inversion: application to multislice perfusion imaging. Magn Reson Med 1997;38:558–564.
38. Yongbi MN, Branch CA, Helpern JA. Perfusion imaging using FOCI RF pulses. Magn Reson Med 1998;40:938–943.
39. Zhang W, Silva AC, Williams DS, Koretsky AP. NMR measurement of perfusion using arterial spin labeling without saturation of macromolecular spins. Magn Reson Med 1995;33:370–376.
40. Wong EC, Buxton RB, Frank LR. Quantitative imaging of perfusion using a single subtraction (QUIPSS and QUIPSS II). Magn Reson Med 1998;39:702–708.
41. Chen Y, Wang DJ, Detre JA. Test-retest reliability of arterial spin labeling with common labeling strategies. J Magn Reson Imaging 2011;33:940–949.
42. Massaro AN, Bouyssi-Kobar M, Chang T, Vezina LG, du Plessis AJ, Limperopoulos C. Brain perfusion in encephalopathic newborns after therapeutic hypothermia. AJNR Am J Neuroradiol 2013;34:1649–1655.
43. Buxton RB, Frank LR, Wong EC, Siewert B, Warach S, Edelman RR. A general kinetic model for quantitative perfusion imaging with arterial spin labeling. Magn Reson Med 1998;40:383–396.
44. Gunther M, Bock M, Schad LR. Arterial spin labeling in combination with a Look-Locker sampling strategy: inflow turbo-sampling EPI-FAIR (ITS-FAIR). Magn Reson Med 2001;46:974–984.
45. Petersen ET, Lim T, Golay X. Model-free arterial spin labeling quantification approach for perfusion MRI. Magn Reson Med 2006;55:219–232.
46. Francis ST, Bowtell R, Gowland PA. Modeling and optimization of Look-Locker spin labeling for measuring perfusion and transit time changes in activation studies taking into account arterial blood volume. Magn Reson Med 2008;59:316–325.
47. Wang DJ, Alger JR, Qiao JX, Gunther M, Pope WB, Saver JL, Salamon N, Liebeskind DS,UCLA Stroke Investigators. Multi-delay multi-parametric arterial spin-labeled perfusion MRI in acute ischemic stroke—comparison with dynamic susceptibility contrast enhanced perfusion imaging. Neuroimage Clin 2013;3:1–7.
48. Gunther M. Highly efficient accelerated acquisition of perfusion inflow series by cycled arterial spin labeling. Proc Intl Soc Mag Reson Med 2007;15:380.
49. Wells JA, Lythgoe MF, Gadian DG, Ordidge RJ, Thomas DL. In vivo Hadamard encoded continuous arterial spin labeling (H-CASL). Magn Reson Med 2010;63:1111–1118.
50. Dai W, Shankaranarayanan A, Alsop DC. Volumetric measurement of perfusion and arterial transit delay using hadamard encoded continuous arterial spin labeling. Magn Reson Med 2013;69:1014–1022.
51. Dixon WT, Sardashti M, Castillo M, Stomp GP. Multiple inversion recovery reduces static tissue signal in angiograms. Magn Reson Med 1991;18:257–268.
52. Ye FQ, Frank JA, Weinberger DR, McLaughlin AC. Noise reduction in 3D perfusion imaging by attenuating the static signal in arterial spin tagging (ASSIST). Magn Reson Med 2000;44:92–100.
53. Bokkers RP, Hernandez DA, Merino JG, Mirasol RV, van Osch MJ, Hendrikse J, Warach S, Latour LL. Whole-brain arterial spin labeling perfusion MRI in patients with acute stroke. Stroke 2012;43:1290–1294.
54. Wang DJ, Alger JR, Qiao JX, et al. The value of arterial spin-labeled perfusion imaging in acute ischemic stroke: comparison with dynamic susceptibility contrast-enhanced MRI. Stroke 2012;43:1018–1024.
55. Maleki N, Dai W, Alsop DC. Optimization of background suppression for arterial spin labeling perfusion imaging. MAGMA 2012;25:127–133.
56. Garcia DM, Duhamel G, Alsop DC. Efficiency of inversion pulses for background suppressed arterial spin labeling. Magn Reson Med 2005;54:366–372.
57. Vidorreta M, Wang Z, Rodriguez I, Pastor MA, Detre JA, Fernandez-Seara MA. Comparison of 2D and 3D single-shot ASL perfusion fMRI sequences. NeuroImage 2012;66C:662–671.
58. Nielsen JF, Hernandez-Garcia L. Functional perfusion imaging using pseudocontinuous arterial spin labeling with low-flip-angle segmented 3D spiral readouts. Magn Reson Med 2013;69:382–390.
59. Gunther M, Oshio K, Feinberg DA. Single-shot 3D imaging techniques improve arterial spin labeling perfusion measurements. Magn Reson Med 2005;54:491–498.
60. Fernandez-Seara MA, Wang Z, Wang J, Rao HY, Guenther M, Feinberg DA, Detre JA. Continuous arterial spin labeling perfusion measurements using single shot 3D GRASE at 3 T. Magn Reson Med 2005;54:1241–1247.
61. Feinberg D, Ramanna S, Guenther M. Evaluation of new ASL 3D GRASE Sequences using parallel imaging, segmented and interleaved k-Space at 3T with 12- and 32-channel coils. In Proceedings of the 10th Annual Meeting of ISMRM, Honolulu, Hawaii, USA, 2002. p. 623.
62. Wang J, Alsop DC, Song HK, Maldjian JA, Tang K, Salvucci AE, Detre JA. Arterial transit time imaging with flow encoding arterial spin tagging (FEAST). Magn Reson Med 2003;50:599–607.
63. Zaharchuk G, Do HM, Marks MP, Rosenberg J, Moseley ME, Steinberg GK. Arterial spin-labeling MRI can identify the presence and intensity of collateral perfusion in patients with moyamoya disease. Stroke 2011;42:2485–2491.
64. Le TT, Fischbein NJ, Andre JB, Wijman C, Rosenberg J, Zaharchuk G. Identification of venous signal on arterial spin labeling improves diagnosis of dural arteriovenous fistulas and small arteriovenous malformations. AJNR Am J Neuroradiol 2012;33:61–68.
65. Wolf RL, Wang J, Detre JA, Zager EL, Hurst RW. Arteriovenous shunt visualization in arteriovenous malformations with arterial spin-labeling MR imaging. AJNR Am J Neuroradiol 2008;29:681–687.
66. Zhou J, Wilson DA, Ulatowski JA, Traystman RJ, van Zijl PC. Two-compartment exchange model for perfusion quantification using arterial spin tagging. J Cereb Blood Flow Metab 2001;21:440–455.
67. Roberts DA, Rizi R, Lenkinski RE, Leigh JS Jr. Magnetic resonance imaging of the brain: blood partition coefficient for water: application to spin-tagging measurement of perfusion. J Magn Reson Imaging 1996;6:363–366.
68. Chalela JA, Alsop DC, Gonzalez-Atavales JB, Maldjian JA, Kasner SE, Detre JA. Magnetic resonance perfusion imaging in acute ischemic stroke using continuous arterial spin labeling. Stroke 2000;31:680–687.
69. Dai W, Robson PM, Shankaranarayanan A, Alsop DC. Sensitivity calibration with a uniform magnetization image to improve arterial spin labeling perfusion quantification. Magn Reson Med 2011;66:1590–1600.
70. Wang J, Qiu M, Constable RT. In vivo method for correcting transmit/receive nonuniformities with phased array coils. Magn Reson Med 2005;53:666–674.
71. Parkes LM. Quantification of cerebral perfusion using arterial spin labeling: two-compartment models. J Magn Reson Imaging 2005;22:732–736.
72. van Gelderen P, de Zwart JA, Duyn JH. Pittfalls of MRI measurement of white matter perfusion based on arterial spin labeling. Magn Reson Med 2008;59:788–795.
73. Zun Z, Shankaranarayanan A, Zaharchuk G. Pseudocontinuous arterial spin labeling with prospective motion correction (PCASL-PROMO). Magn Reson Med 2014;72:1049–1056.
74. Herscovitch P, Raichle ME. What is the correct value for the brain—blood partition coefficient for water? J Cereb Blood Flow Metab 1985;5:65–69.
75. Lu H, Golay X, Pekar JJ, Van Zijl PC. Functional magnetic resonance imaging based on changes in vascular space occupancy. Magn Reson Med 2003;50:263–274.

WOULD YOU LIKE TO POST AN INFORMAL COMMENT ABOUT THIS PAPER, OR ASK THE AUTHORS A QUESTION ABOUT IT?

If so, please visit https://mrm.ismrm.org/ and register for our Magn Reson Med Discourse site (registration is free).

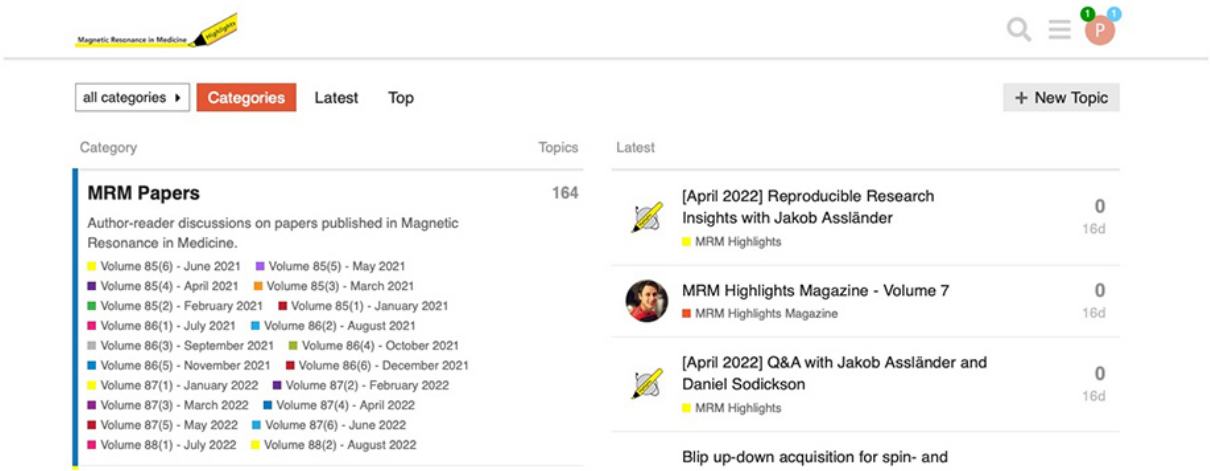

Magn Reson Med is currently listing the top 8 downloaded papers from each issue (including Editor's Picks) for comments and questions on the Discourse web site.

However, we are happy to list this or any other papers (please email mrm@ismrm.org to request the posting of any other papers.)

We encourage informal comment and discussion about Magn Reson Med papers on this site. Please note, however, that a formal errata from the authors should still be submitted in the usual way via our Manuscript Central online submission system.